SMITHSONIAN INSTITUTION
ASTROPHYSICAL OBSERVATORY

Research in Space Science

SPECIAL REPORT

Number 216

ON THE GRADIENT LINE OF THE EARTH'S ZONAL GRAVITATIONAL POTENTIAL

Walter Köhnlein

July 1, 1966

CAMBRIDGE, MASSACHUSETTS 02138

SAO Special Report No. 216

ON THE GRADIENT LINE OF THE EARTH'S ZONAL GRAVITATIONAL POTENTIAL

Walter Köhnlein

Smithsonian Institution
Astrophysical Observatory
Cambridge, Massachusetts 02138

4-66-7

TABLE OF CONTENTS

LIST OF TABLES

LIST OF ILLUSTRATIONS

ABSTRACT

The shape of the gradient line of the earth's zonal gravitational potential is analyzed, and numerical results, such as the radii of curvature, the directional field, etc., are derived from the zonal harmonic coefficients of Kozai and King-Hele.

ON THE GRADIENT LINE OF THE EARTH'S ZONAL GRAVITATIONAL POTENTIAL[1]

Walter Köhnlein[2]

The gradient line of the earth's outer zonal gravitational potential satisfies identically the differential equation

$$\frac{d\vec{x}}{ds} + \frac{\text{grad } U}{|\text{grad } U|} = 0 \quad , \tag{1}$$

which has rotational symmetry in regard to the earth's revolution axis, where U is the earth's outer zonal gravitational potential, s is the arc length of the gradient line, increasing toward outer space, and $\vec{x}$ is the position vector, referred to the mass center of the earth; orientation of x^1, x^2, x^3 is standard. To integrate (1), we transform $\vec{x}$ to a polar coordinate system r, ϕ in a random meridian plane or, for simplicity, to the meridian plane through Greenwich. In this case, the differential equation can be written

[1] This work was supported in part by Grant No. NsG 87 from the National Aeronautics and Space Administration.

[2] Geodesist, Smithsonian Astrophysical Observatory, Cambridge, Massachusetts.

$$
\begin{bmatrix} -\dfrac{\frac{\partial U}{\partial r}}{|\text{grad } U|} & \dfrac{\frac{\partial U}{\partial \phi}}{r|\text{grad } U|} \\ -\dfrac{\frac{\partial U}{\partial \phi}}{r|\text{grad } U|} & -\dfrac{\frac{\partial U}{\partial r}}{|\text{grad } U|} \end{bmatrix} \begin{bmatrix} \cos\phi \\ \sin\phi \end{bmatrix} = \begin{bmatrix} \dfrac{dx^1}{ds} \\ \dfrac{dx^3}{ds} \end{bmatrix} \tag{2}
$$

or

$$
\begin{bmatrix} \dfrac{dr}{ds} & -r\dfrac{d\phi}{ds} \\ r\dfrac{d\phi}{ds} & \dfrac{dr}{ds} \end{bmatrix} \begin{bmatrix} \cos\phi \\ \sin\phi \end{bmatrix} = \begin{bmatrix} \dfrac{dx^1}{ds} \\ \dfrac{dx^3}{ds} \end{bmatrix} \quad . \tag{3}
$$

By comparison of the elements in the left-hand matrices, the differential equation transforms:

$$
\frac{dr}{ds} + \frac{1}{|\text{grad } U|} \frac{\partial U}{\partial r} = 0 \quad , \tag{4}
$$

$$
\frac{d\phi}{ds} + \frac{1}{r^2|\text{grad } U|} \frac{\partial U}{\partial \phi} = 0 \quad . \tag{5}
$$

The arc length s only appears implicitly and hence a simplified version derives if we divide (4) by (5):

$$
\frac{dr}{d\phi} - \frac{1}{r^2} \frac{\partial U}{\partial r} \Big/ \frac{\partial U}{\partial \phi} = 0 \quad . \tag{6}
$$

If we give the potential U in the form

$$U = \frac{GM}{r}\left\{1 - \sum_{n=2}^{\infty}\left(\frac{a}{r}\right)^n J_n P_n(\sin\phi)\right\} \quad , \tag{7}$$

where GM is the gravitational constant × mass of the earth, a is the equatorial radius, J_n are the zonal harmonic coefficients, and P_n are the Legendre's polynomials, the above equation (6) is a function only of r and ϕ, and can be integrated with the help of a special differential equation (Hobson, 1955):

$$\frac{d}{d\phi} P_n(\sin\phi) - \frac{1}{\cos\phi}(n+1)\left[\sin\phi\, P_n(\sin\phi) - P_{n+1}(\sin\phi)\right] = 0 \tag{8}$$

expressing the derivatives of P_n as functions of P_n and P_{n+1}. Equation (8) introduced in (6) and integrated leads to the gradient line in question:

$$\sin\phi + \sum_{n=2}^{\infty}\left(\frac{a}{r}\right)^n \frac{n+1}{n} J_n\left[\sin\phi\, P_n(\sin\phi) - P_{n+1}(\sin\phi)\right] + C = 0 \quad , \tag{9}$$

wherein C is an integration constant, depending on a point r_0, ϕ_0, through which the trajectory runs. The second term (infinite sum) in (9) becomes zero for $r \rightarrow \infty$ and consequently

$$\lim_{r\rightarrow\infty} \phi = \bar{\phi} = \text{arc}\sin(-C), \tag{10}$$

which means that the gradient curve cannot exceed a certain geocentric latitude. Obviously the geocentric radius r in the latitude $\bar{\phi}$ is the asymptote to the gradient line through r_0, ϕ_0.

1. GRADIENT LINE AND ASYMPTOTE

In Table 1 we give the distance

$$D = r \sin |\overline{\phi} - \phi| \tag{11}$$

of a point r, ϕ on the gradient line from its asymptote $\overline{\phi}$ for both the Kozai (1964)[3] and King-Hele[4] coefficients (see Appendix). The initial points r_0, ϕ_0 were taken on a sphere with the radius $r_0 = a, \phi_0$ varying in tens of degrees from 90° to -90°. To obtain the King-Hele values, one has only to add ΔD to the Kozai values D (Kozai) and correspondingly $\Delta\overline{\phi}$ to $\overline{\phi}$ in the case of the asymptote's geocentric latitude.

While D is zero at the poles, it starts increasing toward the middle latitudes and decreases again with $\phi \rightarrow 0$. However, D is by no means constantly zero at the equator but changes in a particular way due to the uneven coefficients J_{2n-1}. This transitional stage near $\phi = 0$ will be further discussed in the last section. In the Northern Hemisphere the gradient line approaches the asymptote from the south, while the opposite is true for the Southern Hemisphere (see Figure 1). Most of the change in D takes places within the first 10,000-km elevation above $r_0 = a$ and tends to zero with $r \rightarrow \infty$.

The difference between the D (Kozai) and D(King-Hele) is hardly noticeable and significant only in lower elevations or near the equator. We see, however, that the Southern Hemisphere shows in

[3] The Kozai coefficients are taken from Kozai (1964). Throughout this paper "Kozai" refers to this paper.

[4] The King-Hele coefficients are taken from King-Hele and Cook (1965) and King-Hele, Cook, and Scott (1965). Throughout this paper "King-Hele" refers to both these papers.

Table 1. Distance of the gradient line from its asymptote (in meters)

H(Km) × 10^3	φ = 90° D	φ = 90° ΔD	φ = 80° D(Kozai)	φ = 80° ΔD	φ = 70° D(Kozai)	φ = 70° ΔD	φ = 60° D(Kozai)	φ = 60° ΔD	φ = 50° D(Kozai)	φ = 50° ΔD
0	0	0	1 762	3	3 315	2	4 471	-1	5 089	-1
0.5			1 635	2	3 075	1	4 147	-1	4 720	-1
1			1 524	2	2 867	1	3 866		4 400	
2			1 343	1	2 526		3 405		3 876	
3			1 200	1	2 257		3 043		3 463	
4			1 085		2 040		2 750		3 130	
5			990		1 861		2 509		2 855	
7			842		1 583		2 134		2 429	
10			688		1 293		1 744		1 984	
20			427		803		1 083		1 232	
30			310		583		785		894	
40			243		457		616		701	
50			200		376		507		577	
60			170		319		431		490	
70			148		278		374		426	
80			131		245		331		376	
90			117		220		297		337	
100	0	0	106		199		269		306	
* $\bar{\phi}°$ | $\Delta\bar{\phi}°$	90°	0	80°.015827	30E-6	70°.029779	17E-6	60°.040165	-9E-6	50°.045715	-6E-6

H(Km) × 10^3	φ = 40° D(Kozai)	φ = 40° ΔD	φ = 30° D(Kozai)	φ = 30° ΔD	φ = 20° D(Kozai)	φ = 20° ΔD	φ = 10° D(Kozai)	φ = 10° ΔD	φ = 0° D(Kozai)	φ = 0° ΔD
0	5 095	1	4 487	1	3 338	-1	1 784	-3	7.550	1.342
0.5	4 725		4 161	1	3 095	-1	1 653	-2	6.695	0.735
1	4 405		3 879		2 885	-1	1 540	-1	5.900	0.437
2	3 880		3 416		2 540		1 355		4.623	0.189
3	3 467		3 052		2 269		1 210		3.704	0.099
4	3 133		2 758		2 050		1 093		3.031	0.060
5	2 858		2 516		1 870		997		2.525	0.041
7	2 431		2 140		1 590		847		1.832	0.022
10	1 986		1 748		1 299		692		1.227	0.011
20	1 233		1 085		806		429		0.476	0.004
30	894		787		584		311		0.251	0.002
40	701		617		458		244		0.155	0.001
50	577		508		377		201		0.105	0.001
60	490		431		320		171		0.076	0.001
70	426		375		278		148		0.058	
80	377		331		246		131		0.045	
90	338		297		220		117		0.036	
100	306		269		200		106		0.030	
* $\bar{\phi}°$ | $\Delta\bar{\phi}°$	40°.045769	5E-6	30°.040305	9E-6	20°.029982	-8E-6	-10°.016024	-21E-6	0°.000068	12E-6

H(Km) × 10^3	φ = -90° D	φ = -90° ΔD	φ = -80° D(Kozai)	φ = -80° ΔD	φ = -70° D(Kozai)	φ = -70° ΔD	φ = -60° D(Kozai)	φ = -60° ΔD	φ = -50° D(Kozai)	φ = -50° ΔD
0	0	0	1 775	4	3 338	2	4 495	-1	5 107	0
0.5			1 646	2	3 094	1	4 167	-1	4 736	
1			1 534	1	2 883	1	3 883		4 415	
2			1 350	1	2 538		3 419		3 887	
3			1 206		2 266		3 053		3 472	
4			1 089		2 047		2 759		3 137	
5			993		1 867		2 516		2 861	
7			845		1 587		2 139		2 433	
10			690		1 296		1 747		1 987	
20			428		804		1 084		1 233	
30			310		583		786		894	
40			243		457		617		701	
50			200		376		507		577	
60			170		320		431		490	
70			148		278		374		426	
80			131		246		331		377	
90			117		220		297		337	
100	0	0	106		199		269		306	
$\bar{\phi}°$ | $\Delta\bar{\phi}°$	-90°	0	-80°.015948	-36E-6	-70°.029985	-17E-6	-60°.040383	15E-6	-50°.045875	1E-6

H(Km) × 10^3	φ = -40° D(Kozai)	φ = -40° ΔD	φ = -30° D(Kozai)	φ = -30° ΔD	φ = -20° D(Kozai)	φ = -20° ΔD	φ = -10° D(Kozai)	φ = -10° ΔD	φ = 0° D(Kozai)	φ = 0° ΔD
0	5 106	1	4 492	0	3 331	1	1 770	-2	see above	
0.5	4 735	1	4 165		3 089	1	1 641	-1		
1	4 414	1	3 882		2 880		1 530	-1		
2	3 887		3 418		2 536		1 347			
3	3 473		3 054		2 266		1 204			
4	3 138		2 759		2 048		1 088			
5	2 862		2 517		1 868		992			
7	2 434		2 141		1 588		844			
10	1 988		1 748		1 298		690			
20	1 234		1 085		806		429			
30	895		787		584		311			
40	702		617		458		244			
50	577		508		377		201			
60	490		431		320		170			
70	426		375		278		148			
80	377		331		246		131			
90	338		297		221		117			
100	306		269		200		106			
$\bar{\phi}°$ | $\Delta\bar{\phi}°$	-40°.045871	-5E-6	-30°.040349	-2E-6	-20°.029925	-7E-6	-10°.015898	18E-6		

*E-6 means × 10^{-6}

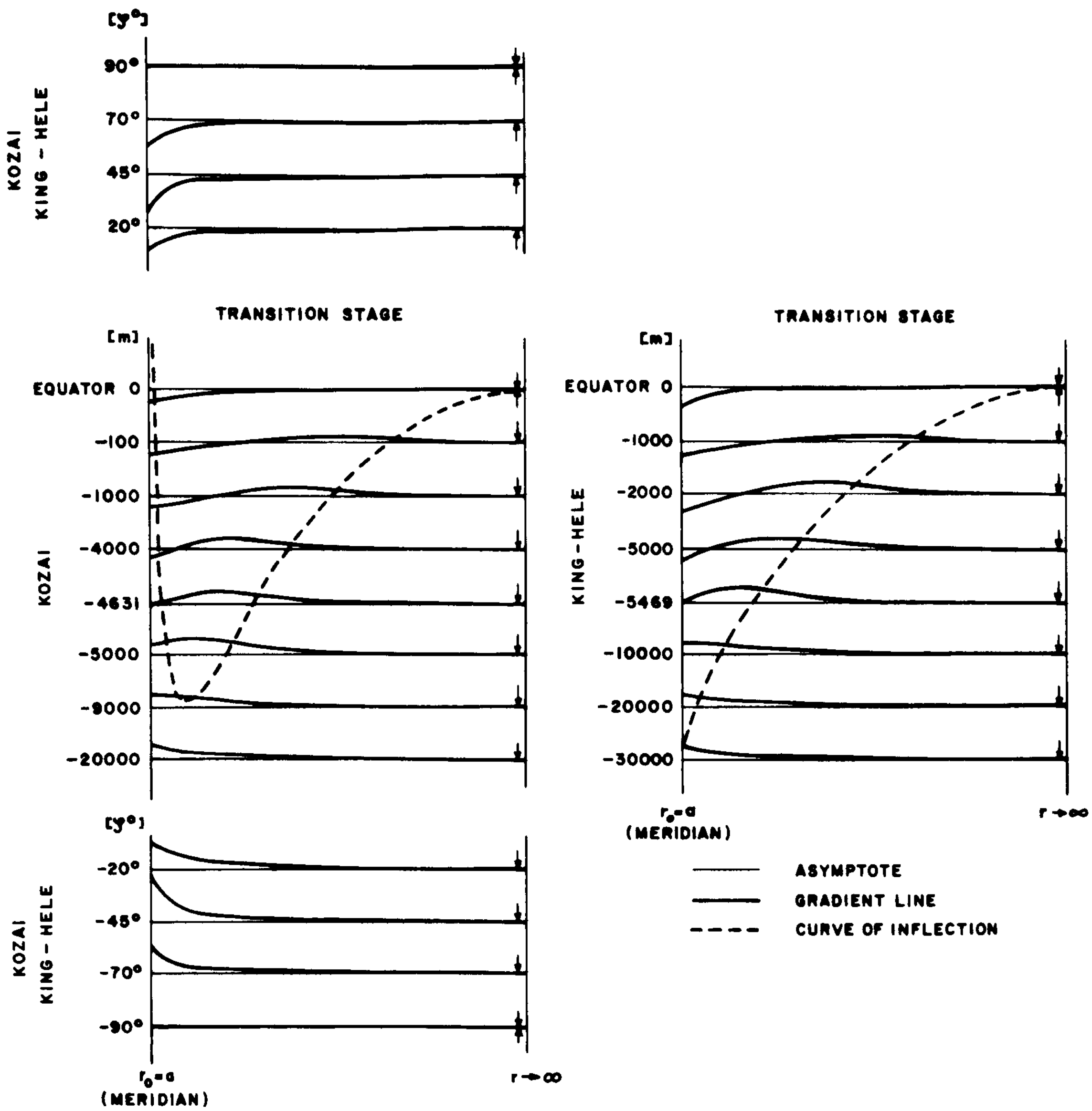

Figure 1. Shape of the gradient line.

both a stronger curved gradient line between the poles and $|\phi| \sim 30°$ than the Northern Hemisphere. From $|\phi| \sim 20°$ on, this changes toward the equator, where D becomes larger at the Northern Hemisphere compared to D at the Southern Hemisphere. If we plot the distance D as a function of the geocentric latitude ϕ, we obtain a sinusoidal-like curve with maxima at the middle latitudes and minima at the poles and near the equator. The amplitude decreases hereby from ~ 5.1 km at the earth's surface to 0.3 km at 100,000-km elevation and to 0 km at $H \to \infty$.

A further insight into the straightness of a gradient line can be obtained if we compare its length up to ∞ with the corresponding projection on its asymptote. Starting from the arc length s_{12} between two curve points $Q_1(r_1, \phi_1)$, $Q_2(r_2, \phi_2)$ of the gradient line

$$s_{12} = \int_{r_1}^{r_2} \sqrt{1 + \left(r \frac{d\phi}{dr}\right)^2}\, dr \quad , \tag{12}$$

we obtain the projection on its asymptote

$$\bar{s}_{12} = r_2 \cos(\bar{\phi} - \phi_2) - r_1 \cos(\bar{\phi} - \phi_1) \quad , \tag{13}$$

and the difference Δs for Q_1 on $r_1 = a$, and Q_2 on $r_2 \to \infty$,

$$\Delta s = \lim_{\substack{r_1 = a \\ r_2 \to \infty}} (s_{12} - \bar{s}_{12}) \quad . \tag{14}$$

Without going further into details, Figure 2 shows the values for Δs as a function of ϕ. As expected, we get analogous results to D, namely, zero values at the poles (where the gradient line is a straight line) that increase to their maxima of ~ 0.7m in middle latitudes and drop to very small values at or near the equator. Actually the main contribution in Δs comes again from the section within 10,000-km elevation above the earth's surface, while for higher elevations $s_{12} - \bar{s}_{12}$ tends quickly toward zero as can be easily seen from equation (12).

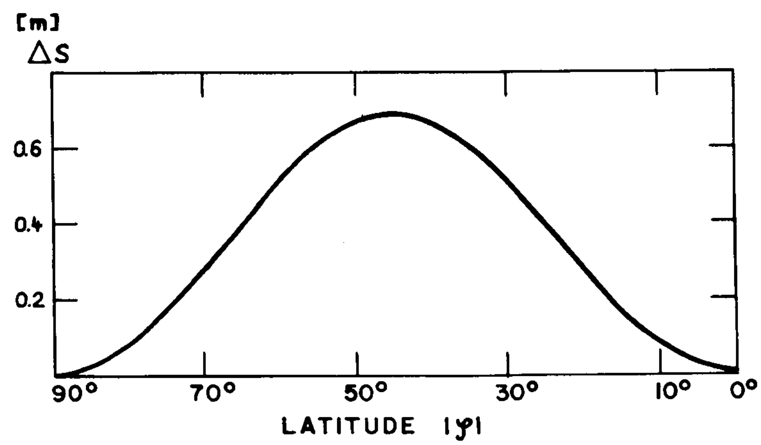

Figure 2. Difference between the total length of the gradient line and its projection on its asymptote.

2. DIRECTION FIELD AND CURVATURE

Equation (1) gives the direction of the tangent in each point of the gradient line. Intersecting it with the corresponding geocentric radius vector leads to the angle

$$\nu = \text{arc sin} \frac{1}{r|\text{grad } U|} \left| \frac{\partial U}{\partial \phi} \right| \quad , \tag{15}$$

which represents the directional field of the differential equation (1) in a spherical coordinate system (Köhnlein, 1966). In Table 2 the ν (Kozai) are directly given, while the ν (King-Hele) follow again by adding $\Delta\nu$ to ν(Kozai). The different elevations H refer to the same geocentric latitude, and hence the values ν do not lie on the same gradient line.

The pattern of the numerical results is unchanged from the previous ones: zeros at the poles, maxima in middle latitudes, and minima around the equator. Figure 3 shows the points relative to the equator $\phi = 0$, where the tangent is perpendicular to the revolution axis. For Kozai's coefficients the curve moves at first slightly southward and approaches afterward asymptotically the equator $\phi = 0$, while for the King-Hele coefficients the curve drops down asymptotically right from the beginning.

Table 2. Direction field

$\phi°$ \ ν	H = 0		H = 1,000 km		H = 10,000 km		H = 100,000 km	
	ν (Kozai)	$\Delta\nu$	ν (Kozai)	$\Delta\nu$	ν (Kozai)	$\Delta\nu$	ν (Kozai)	$\Delta\nu$
90	0"	0"	0"	0"	0"	0"	0"	0"
80	1'53".48	0".89	1'25".08	0".27	17".3390	0".0011	0".4117	0".0000
70	3'34".03	0".46	2'50".14	0".15	32".5925	0".0014	0".7738	
60	4'49".04	-0".37	3'36".02	-0".08	43".9244	0".0010	1".0426	
50	5'28".83	-0".16	4' 5".86	-0".06	49".9686	0".0002	1".1857	
40	5'29".33	0".12	4' 6".14	0".05	49".9939	-0".0004	1".1857	
30	4'49".99	0".32	3'36".78	0".09	43".9922	-0".0011	1".0428	
20	3'35".97	-0".10	2'41".36	-0".08	32".6811	-0".0014	0".7741	
10	1'56".16	-0".71	1'26".36	-0".18	17".4195	-0".0007	0".4120	
0	0' 0".59	0".40	0' 0".47	0".10	0".0460	0".0006	0".0002	
-10	1'54".61	-0".52	1'25".48	-0".16	17".3424	-0".0014	0".4117	
-20	3'35".29	0".41	2'40".97	0".05	32".6446	-0".0013	0".7740	
-30	4'50".86	-0".06	3'37".09	0".04	44".0111	-0".0005	1".0429	
-40	5'30".15	0".14	3' 6".82	0".04	50".0683	0".0002	1".1860	
-50	5'30".16	0".06	4' 6".93	-0".02	50".0838	0".0008	1".1861	
-60	4'51".71	-0".61	3'37".57	-0".12	44".0540	0".0012	1".0431	
-70	3'36".61	0".48	2'41".65	0".14	32".7044	0".0015	0".7742	
-80	1'54".92	1".12	1'25".97	0".32	17".4038	0".0011	0".4120	0".0000
-90	0"	0"	0"	0"	0"	0"	0"	0"

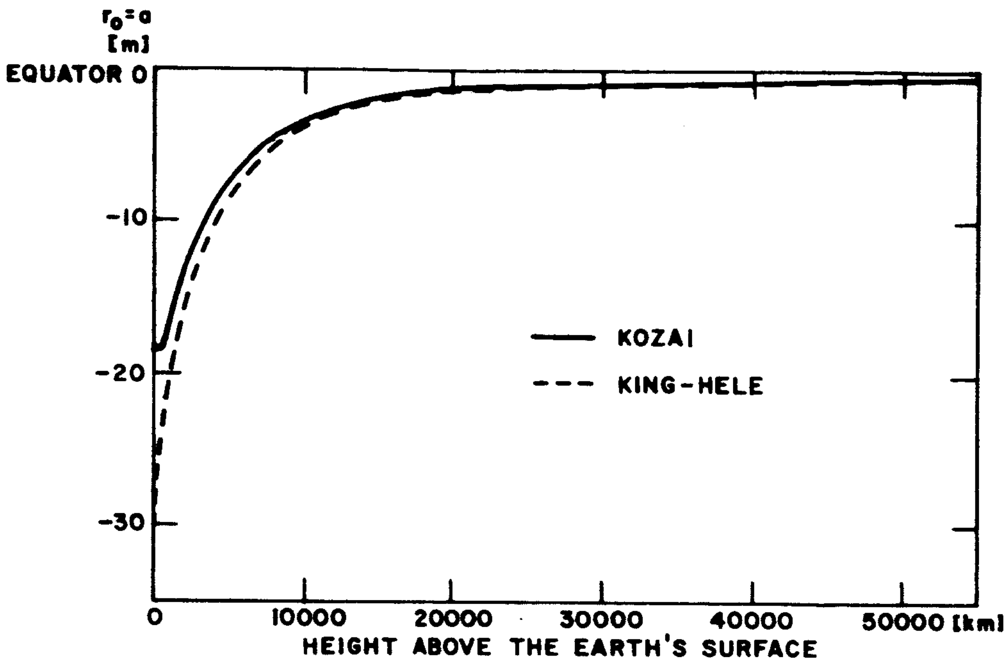

Figure 3. Curve locus: tangent.

The variation of the directional field leads to the curvature of the gradient lines. Differentiating equation (1) with respect to s, one gets the radius of curvature

$$\rho = \frac{1}{\sqrt{\frac{d^2\vec{x}}{ds^2} \frac{d^2\vec{x}}{ds^2}}} \quad , \tag{16}$$

as shown in Table 3 for elevations up to 100,000 km. Of particular interest is the area around the equator. While the radius of the curvature, computed from the King-Hele coefficients, increases steadily

Table 3. Radius of curvature (km)

$\phi°$ \ ρ	H = 0		H = 1,000 km		H = 10,000 km		H = 100,000 km	
	ρ (Kozai)	$\Delta\rho$	ρ (Kozai)	$\Delta\rho$	ρ (Kozai)	$\Delta\rho$	ρ (Kozai)	$\Delta\rho$
90	∞	0	∞	0	∞	0	∞	0
80	119E5*	- 7E5	181E5	- 4E5	195E6	0	533E8	0
70	620E4	- 9E4	955E4	- 6E4	104E6	0	284E8	0
60	454E4	5E4	705E4	3E4	770E5	0	211E8	0
50	402E4	1E4	620E4	2E4	677E5	0	185E8	0
40	400E4	- 1E4	619E4	0	676E5	0	185E8	0
30	456E4	- 4E4	704E4	- 3E4	768E5	0	210E8	0
20	612E4	- 2E4	941E4	2E4	103E6	0	283E8	0
10	108E5	6E5	173E5	3E5	193E6	0	532E8	0
0	227E7	-183E7	230E7	-126E7	370E8	-7E8	647E11	-4E11
-10	113E5	3E5	177E5	2E5	195E6	0	533E8	0
-20	620E4	- 14E4	947E4	- 5E4	104E6	0	284E8	0
-30	446E4	4E4	699E4	0	767E5	0	210E8	0
-40	401E4	- 2E4	618E4	- 1E4	674E5	0	185E8	0
-50	403E4	- 2E4	617E4	0	674E5	0	185E8	0
-60	441E4	9E4	693E4	4E4	766E5	0	210E8	0
-70	600E4	- 10E4	932E4	- 6E4	103E6	0	283E8	0
-80	116E5	- 8E5	177E5	- 5E5	194E6	0	532E8	0
-90	∞	0	∞	0	∞	0	∞	0

*E5 means $\times 10^5$

with higher elevations, the radius ρ (Kozai) increases at first, then decreases at around 1,000 km, then starts increasing again (ρ is bigger at 1,000 km than ρ at sea level, however smaller than ρ at 100 km elevation). This behavior of the gradient line near $\phi = 0$ is due to the position of its inflection points (where $\rho = \infty$) as shown in Figure 4 and discussed below.

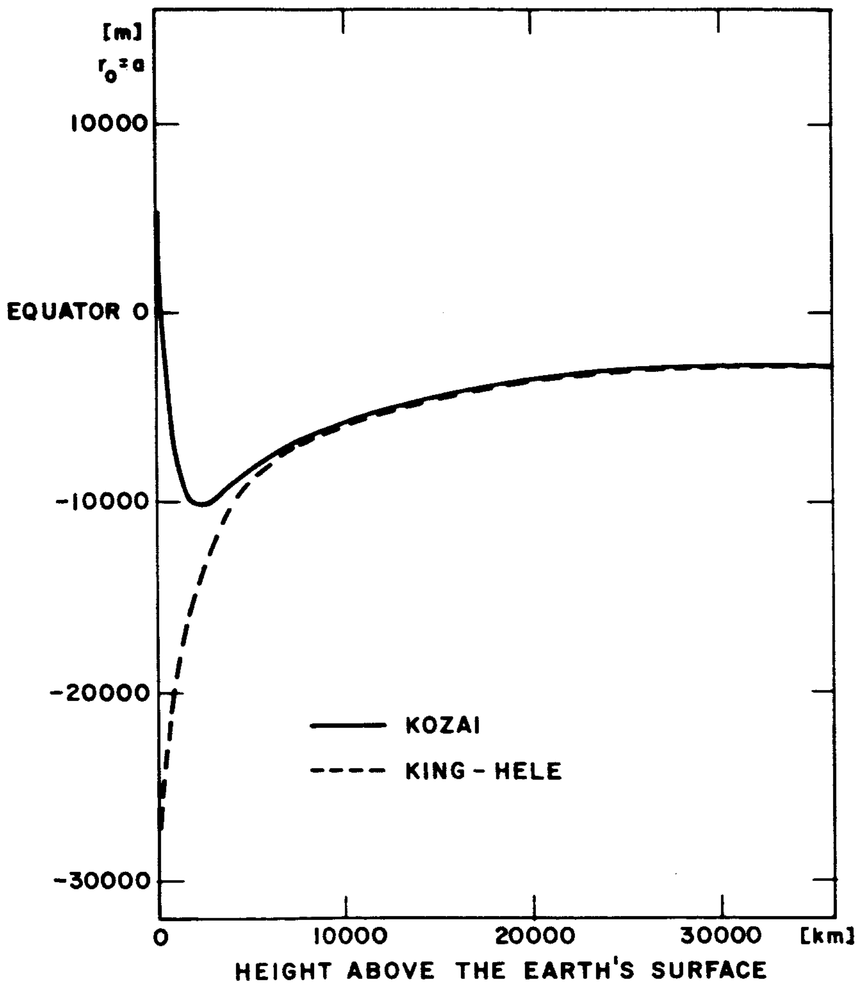

Figure 4. Curve of inflection.

3. BEHAVIOR OF THE GRADIENT LINE AROUND THE EQUATOR

The uneven harmonic coefficients of the earth's gravitational field cause a certain disturbance in the run of the gradient line near the equator. While in the Northern and Southern Hemispheres the gradient lines are bent away from the poles (at the poles they coincide with the revolution axis x^3) and approximate smoothly their asymptotes with higher elevations, this behavior changes definitely during the transition stage near $\phi = 0$. Here the curves have points of inflection satisfying the equation

$$\frac{d^2x^3}{ds^2} - \frac{d^2x^1}{ds^2}\frac{dx^3}{dx^1} = 0 \quad , \tag{17}$$

which is plotted in Figure 4 for both the harmonic coefficients. While Kozai's J_n produce in general two points of inflection in the considered area, the King-Hele harmonics lead to only one inflection point per gradient line, however over a wider range.

In Figure 1 we show schematically the shape of the gradient lines relative to their asymptotes. The arrows point out the directions from which the asymptote is approached at infinity. Except at the poles we have only one further point where a change in the approach takes place: The equatorial point at infinity. This is due to the combined asymptotic approach of the gradient line and the curve of inflection.

The width of the transition stage around the equator amounts in Kozai's and King-Hele's cases to $\sim 15,000$ m and 30, 000 m, respectively, along $r_0 = a$. As shown in Figure 1 the gradient line bends and oscillates here relative to its asymptote before it assumes the monotone approach typical outside of this transition zone.

Perhaps one point needs some additional explanation, namely where the initial point Q_1 (on $r_0 = a$) falls together with its asymptote. From the following expression we find its geocentric latitude $\bar{\phi} = \phi_0$:

$$\sum_{n=2}^{\infty} \left(\frac{a}{r}\right)^n \frac{\cos\phi}{n} J_n \frac{d\, P_n(\sin\phi)}{d\phi} = 0 \quad ,$$

with $r_0 = a$ satisfying equation (9) both at $r = a$ and $r \to \infty$. For Kozai's set of harmonic coefficients we get:

$$\phi_0 \approx -2'29''.7 \text{ (or } -4631 \text{ m southward of the equator along } r = a),$$

and analogously for King-Hele's set:

$$\phi_0 \approx -2'56''.8 \text{ (or } -5469 \text{ m southward of the equator along } r = a).$$

4. ACKNOWLEDGMENTS

I am indebted to Dr. C. A. Lundquist for reading the paper and to Messrs. M. Stein and J. Maguire for their skillful programming work.

5. REFERENCES

HOBSON, E. W.

1955. The Theory of Spherical and Ellipsoidal Harmonics. Chelsea Publishing Co., New York, 500 pp.

KING-HELE, D. G., AND COOK, G. E.

1965. The even zonal harmonics of the earth's gavitational potential. Geophys. Journ. Roy. Astron. Soc., vol. 10, no. 1, pp. 17-29.

KING-HELE, D. G., COOK, G. E., AND SCOTT, D. W.

1965. The odd zonal harmonics in the earth's gravitational potential. Royal Aircraft Establishment Tech. Rep. No. TR-65123, 43 pp.

KÖHNLEIN, W.

1966. Geometric structure of the earth's gravitational field as derived from artificial satellites. Smithsonian Astrophys. Obs. Spec. Rep. No. 198, 109 pp.

KOZAI, Y.

1964. New determination of zonal harmonics coefficients of the earth's gravitational potential. Smithsonian Astrophys. Obs. Spec. Rep. No. 165, 38 pp.

APPENDIX

CONSTANTS AND COEFFICIENTS USED

a $= 6\ 378\ 165$ m, earth's equatorial radius.

GM $= 3.986\ 032 \times 10^{20}\ \mathrm{cm}^3\ \mathrm{sec}^{-2}$, gravitational constant $\times$ mass of the earth.

Harmonic Coefficients

	KOZAI	KING-HELE
J_2	1082.645×10^{-6}	1082.64×10^{-6}
J_3	-2.546×10^{-6}	-2.56×10^{-6}
J_4	-1.649×10^{-6}	-1.52×10^{-6}
J_5	-0.210×10^{-6}	-0.15×10^{-6}
J_6	0.646×10^{-6}	0.57×10^{-6}
J_7	-0.333×10^{-6}	-0.44×10^{-6}
J_8	-0.270×10^{-6}	0.44×10^{-6}
J_9	-0.053×10^{-6}	0.12×10^{-6}
J_{10}	-0.054×10^{-6}	
J_{11}	0.302×10^{-6}	
J_{12}	-0.357×10^{-6}	
J_{13}	-0.114×10^{-6}	
J_{14}	0.179×10^{-6}	

NOTICE

This series of Special Reports was instituted under the supervision of Dr. F. L. Whipple, Director of the Astrophysical Observatory of the Smithsonian Institution, shortly after the launching of the first artificial earth satellite on October 4, 1957. Contributions come from the Staff of the Observatory.

First issued to ensure the immediate dissemination of data for satellite tracking, the reports have continued to provide a rapid distribution of catalogs of satellite observations, orbital information, and preliminary results of data analyses prior to formal publication in the appropriate journals. The Reports are also used extensively for the rapid publication of preliminary or special results in other fields of astrophysics.

The Reports are regularly distributed to all institutions participating in the U. S. space research program and to individual scientists who request them from the Publications Division, Distribution Section, Smithsonian Astrophysical Observatory, Cambridge, Massachusetts 02138.